Numerical analysis of the velocity of abrasive particles in an abrasive blasting device.

Josef Vosahlo[1] and Pavel Srb[1]

[1]Institute for Nanomaterials, Advanced Technologies and Innovation, Technical University of Liberec, Studentska 2, Liberec 461 17, Czech Republic
josef.vosahlo@tul.cz

Abstract. The article deals with by using numerical analysis of abrasive particle velocity in blast technology. Blasting technology is an important industrial process that allows the application of materials to surfaces using high pressure or air velocity. The velocity of abrasive particles is a key parameter of the blasting process. For the high performance of blasting equipment, it is necessary for the abrasive particles to hit the treated surface at a given angle and speed. The velocity distribution of individual abrasive particles must be as uniform as possible. A two-dimensional FEM model of the interior space of the blasting equipment was created, where the flow of abrasive particles of various sizes was simulated. The numerical simulation was performed for various input parameters, including the use of different shapes of blades of the blast wheel. The obtained results will lead to the design of an innovative blasting device with higher performance.

Keywords: Numerical Simulation, Blasting Technology, Blasting Wheel, Abrasive Particles

1 Introduction

Abrasive blasting has wide applications in various industries such as engineering, automotive, construction, and others. The main applications include surface cleaning, removal of impurities, surface preparation for painting, and increasing the roughness of surfaces. With the advancement in the development of materials and techniques, the blasting technology is constantly being improved and finds new applications to solve industrial challenges and needs.

However, insufficient treatment can lead to premature corrosion under the coating due to the penetration of moisture and residual salts, which can cause structural failure [1]. Blasting is a commonly used method of surface treatment, with parameters such as nozzle diameter, type of abrasive, and blasting pressure significantly affecting surface properties. Research has shown that factors such as abrasive material and particle shape affect surface properties, including roughness and the introduction of secondary impurities [2, 3]. Studies [4, 5] also reveal a relationship between blasting conditions and corrosion behavior in different environments. In addition, abrasive blasting has found applications beyond steel structures, for instance in the processing

M. Petr et al. (eds.), *62nd International Conference of Machine Design Departments (ICMD 2022)*,
Atlantis Highlights in Engineering 28,
https://doi.org/10.2991/978-94-6463-423-5_16

of ceramics and semiconductors, thanks to minimal thermal effects and low cutting forces.

In abrasive blasting, a mixture of abrasive grains and pressurized air is used to achieve the desired quality and profile of the surface. The process consists of three main phases: acceleration of grains in the blasting hose, spraying the nozzle towards the work piece, and the impact of grains on the surface for material removal. Various studies [4 - 7] focus on understanding the principles of abrasive blasting, optimizing operating parameters, and predicting outcomes such as hose erosion and surface cleanliness. Additionally, research [8, 9] has examined the influence of the movement modes of the blasting gun and speed on the quality and productivity of blasting.

The rotating head is a key component of blasting machines, which drives projectiles onto the surface of the work piece. High-speed rotating blades in the head of the rotary wheel face dynamic impact forces from the projectiles, leading to their wear and potential breakage.

The aim of this study was to analyze the distribution of speeds of abrasive particles during the blasting process. The obtained results will lead to improvements in the design of blasting equipment, increasing its efficiency and reducing its energy consumption.

2 Materials and Methods

For the creation of the numerical simulation, the ANSYS system was utilized, which is a multiphysics simulation program that allows for simulations including physical and structural properties, vibrations, fluid flow, heat transfer, or electromagnetic properties. With the help of the multiphysics interface of the ANSYS system, these simulations can be conducted individually or all can be incorporated into a single simulation. This work addresses the airflow with a mixture of added particles that simulate an abrasive. The Fluent module has been used for this purpose.

2.1 Flow model

For this study, the K-epsilon turbulence model [10] was utilized, which is one of the most commonly used and well-known models in practice (equations 1 and 2). This is primarily due to its robustness, simplicity of computation, and yet sufficient accuracy. However, its use requires that the flow be fully turbulent.

$$\frac{\partial}{\partial t}(pk) + \frac{\partial}{\partial x_i}(pku_i) = \frac{\partial}{\partial x_j}\left[\left(\mu + \frac{\mu_t}{\sigma_k}\right)\frac{\partial k}{\partial x_j}\right] + G_k + G_b - p\varepsilon - Y_M + S_k \quad (1)$$

$$\frac{\partial}{\partial t}(p\varepsilon) + \frac{\partial}{\partial x_i}(p\varepsilon u_i) = \frac{\partial}{\partial x_j}\left[\left(\mu + \frac{\mu_t}{\sigma_\varepsilon}\right)\frac{\partial \varepsilon}{\partial x_j}\right] + G_{1\varepsilon}\frac{\varepsilon}{k}(G_k + C_{3\varepsilon}G_b) - C_{2\varepsilon}\frac{\varepsilon^2}{k} + S_\varepsilon \quad (2)$$

where

G_k is the generation of turbulence kinetic energy k due to mean velocity gradients

G_b is the generation of turbulence kinetic energy k due to buoyancy

Y_m represents the contribution from fluctuating dilatations in compressible turbulent flow to the total dissipation $C_{1\varepsilon}$, $C_{2\varepsilon}$, $C_{3\varepsilon}$ are model constants

$\sigma_k, \sigma_\varepsilon$ are the model constants—turbulent Prandtl numbers for k a ε

S_k, S_ε are user-defined resource members. The turbulent viscosity is calculated from the relation:

$$\mu_t = \rho C_\mu \frac{k^2}{\varepsilon} \tag{3}$$

where

C_μ is a model constant.

2.2 Geometry and mesh

For this study, two-dimensional geometry was utilized primarily due to the computational demands of the model. Initially, the 3D CAD geometry of a standard abrasive blasting device was simplified by removing elements that do not directly participate in the airflow with abrasive particles. Subsequently, the geometry was converted into 2D and a finite element mesh was created. Fluent calculates the velocities, pressures, particle motions, and other quantities for each individual cell in the mesh. Depending on the detail of the mesh grid, the results can be distorted (for too coarse a mesh) or lead to unfeasibly demanding and lengthy simulations (for very detailed meshes). The size of the elements was chosen such that the entire model would have approximately 22,000 elements; with this number of elements, the computer is capable of performing the calculation without errors, and at the same time, the mesh is sufficiently optimized (Fig. 1). The mesh is composed of quadrilateral elements and is refined (0.4 mm) in the area where the abrasive particles enter (center of the wheel).

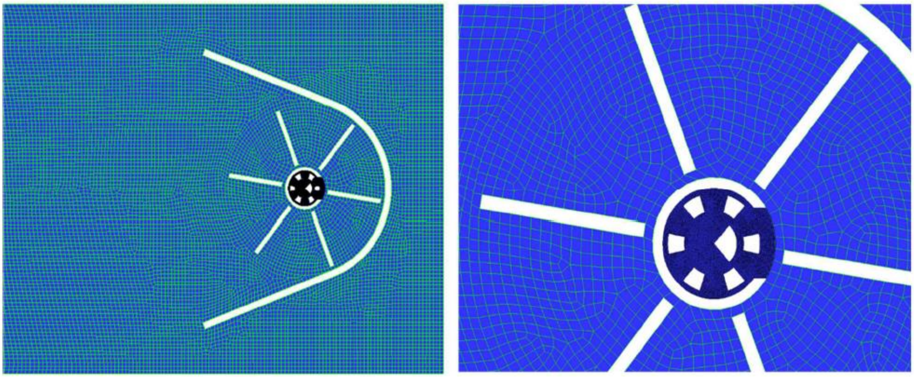

Fig. 1. Optimized finite element mesh of the entire model (left), detail (right).

2.3 Materials and boundary conditions

The material properties were set as follows: the flowing fluid was set to air from the Fluent database with parameters of density 1.225 kg/m³ and viscosity 1.789e-5 kg/(m·s). The other parts of the device are made of steel with a density of 7850 kg/m³. The last material was the abrasive with a density of 7000 kg/m³. Furthermore, it was necessary to set Cell zone conditions for different areas of the mesh, determining whether they are solid or a flowing medium. To introduce the rotation of the blasting turbine, a boundary condition of 2900 rpm rotational speed was implemented. Since the abrasive particles fell due to gravity into the separator, there was no need to set an inlet velocity. This parameter was therefore set to a zero value. The pressure at the outlet was set to zero, which corresponds to the pressure difference relative to atmospheric pressure (initial gauge pressure). Output parameters were specified for particles leaving the bounded space. When particles come into contact with the wall of the blasting turbine, it was necessary to set a contact condition (reflect) so that the particles would respond to the contact conditions associated with the rebound speed upon impact with the wall. For the inlet entry, the turbulence specification method must be set to intensity and hydraulic diameter. Given that an inlet velocity is absent and therefore no turbulent flow occurs in this area, this value was left at zero.

3 Results and Discussion

To track the trajectories of individual particles, the calculation step would have to be set to 5e-5 seconds, which would lead to a very high computational demand. Therefore, a different approach was selected to evaluate the distribution of particle velocities. The calculation step was chosen to be 0.1 seconds. The blasting turbine makes 4.8 revolutions in 0.1 seconds, so the trajectory of each abrasive particle is not tracked, but the velocities of particles in the 0.1-second interval are monitored. This solution allowed for the observation of 30 seconds of the turbine's operation. The output from the Fluent numerical simulation system was 300 graphic files (Fig. 2) in raster graphics for the 30 seconds of the turbine's operation.

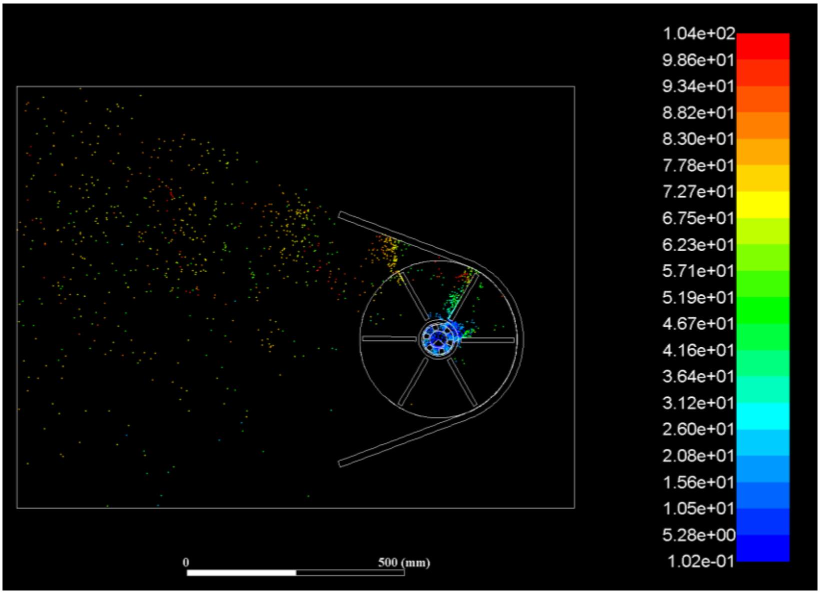

Fig. 2 Distribution of abrasive particle velocities at time t = 1 s.

The graphic files were exported in a predefined resolution of 1920x1080 pixels and TrueColors quality with a bit depth of 24 bits. These were further processed by an evaluation application developed in the LabView environment (Fig. 3). The application proceeded as follows: after loading an image, it evaluated the color of the pixel in the first row and first column; if the color value was black, it was not compared with the scale and not counted. If the color was different, it was compared with the scale, evaluated, assigned to the corresponding velocity interval, and counted as a valid particle. Next, the pixel value in the first row and second column was evaluated, and so on. After completing the evaluation of the image, the next one was loaded, and the procedure was repeated. From these obtained intervals with a known number of particles and the total number of particles, the percentage of particles at a given speed was calculated, which is then presented in graphs and discussed.

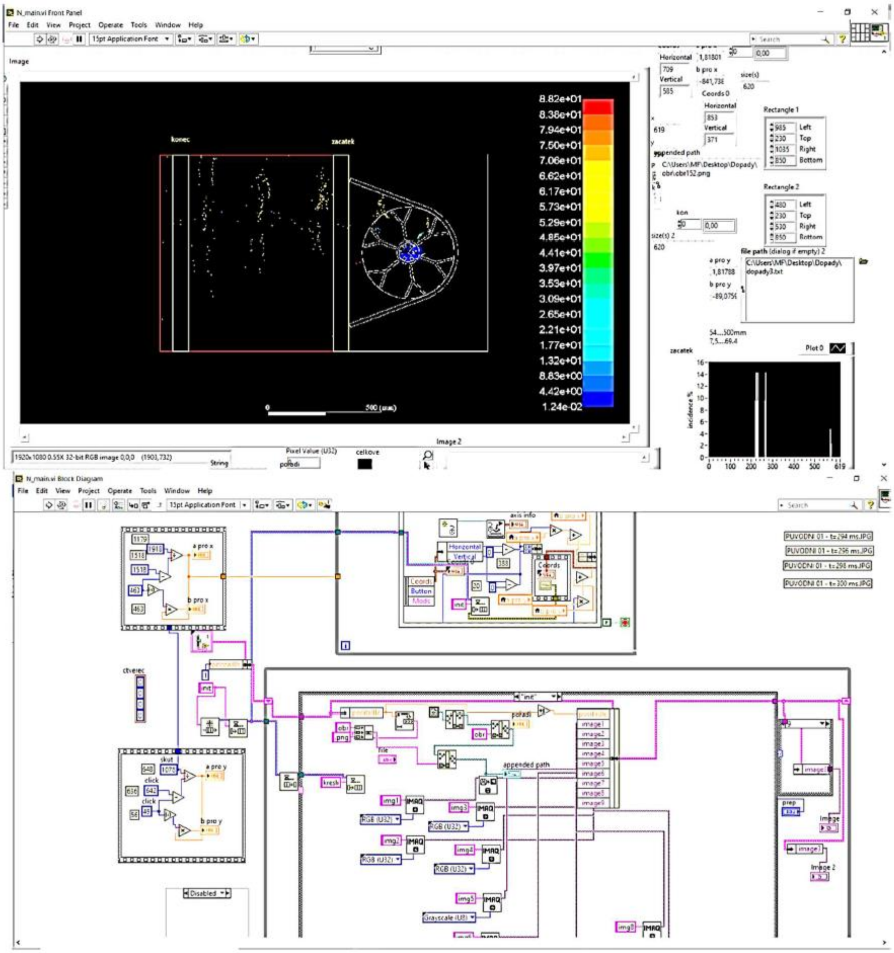

Fig. 3. Evaluating images using LabView.

To remove impurities from a product (such as burrs, molding sand, rust, paint, etc.), it is desirable for the particles that impact the surface of the cleaned product to have the highest possible energy. Given the defined and unchangeable volume and density of the abrasive, the energy of the particle can be influenced by its velocity. In the case of a blasting turbine, this velocity is affected by air resistance and the initial momentum imparted to the particle by the blade. For maximum cleaning effect, it is ideal for the particles to hit as large an area as possible at the highest possible velocity. For straight blades of the turbine, the analyzed velocity of particles was presented as a percentage representation of particles with a corresponding velocity (falling within a certain velocity interval) relative to all particles. This display is shown in the following graph (Fig. 4). Here, the velocity of particles is divided into twenty intervals occurring between the maximum and minimum velocities, according to the scale on the given image. In the graphs, these intervals are divided in the range of 0–119 m/s. To visualize this data accurately, the graph (Fig. 4) would typically be a histogram or a distribution plot, where the x-axis represents the velocity intervals and the y-axis represents the percentage of particles within each interval. Each bar or point on the graph correlates to an interval of particle velocities and shows the fraction or percentage of the total particles that fall within that velocity range. By analyzing the distribution of particle velocities, one can determine the effectiveness of the cleaning process and adjust the turbine operation as needed to ensure that particles have sufficient energy to clean the product surface effectively.

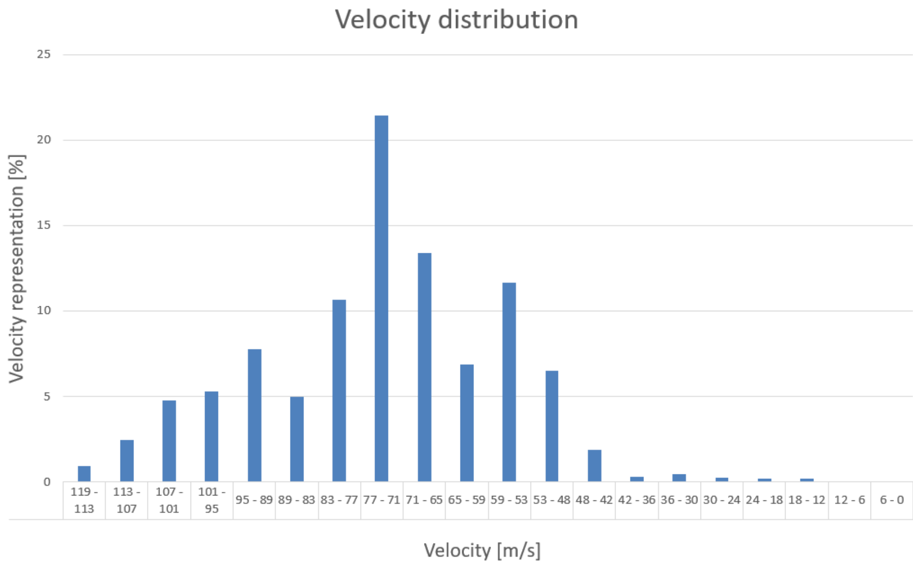

Fig. 4. Distribution of abrasive particle velocities after 30 s of steady running.

4 Conclusions

A simulation was created to track the trajectory of abrasive particles passing through a blasting apparatus. The simulations were conducted for various abrasive parameters. The results show a very good agreement with real experiments. The results of the conducted simulation will be used for further development of the blasting equipment. Modifications to the shape of the blades will be proposed so that the distribution of particle velocity at the output of the blasting apparatus is as uniform as possible.

References

1. Kim, A.; Kainuma, S.; Yang, M. Surface Characteristics and Corrosion Behavior of Carbon Steel Treated by Abrasive Blasting. Metals 2021, 11, 2065. https://doi.org/10.3390/met11122065
2. N. Liu et al., "Modelling of abrasive blasting process from viewpoint of energy exchange," 2018 IEEE 23rd International Conference on Emerging Technologies and Factory Automation (ETFA), Turin, Italy, 2018, pp. 488-492, doi: 10.1109/ETFA.2018.8502548.
3. Y. Zhang, S. Wang, Y. Pan, T. Zhang, Z. Jiang and X. Fu, "Research on Optimization Design of Shot Blasting Machine Blade Based on Modal Analysis," 2021 Global Reliability and Prognostics and Health Management (PHM-Nanjing), Nanjing, China, 2021, pp. 1-5, doi: 10.1109/PHM-Nanjing52125.2021.9612963.
4. Tianyi Zhang et al., Study on the dynamic fatigue performance of shot blasting machine's blades based on modal analysis, 2021 J. Phys.: Conf. Ser. 1948 012214
5. M. Achtsnick, P.F. Geelhoed, A.M. Hoogstrate, B. Karpuschewski, Modelling and evaluation of the micro abrasive blasting process, Wear, Volume 259, Issues 1–6, 2005, Pages 84-94, ISSN 0043-1648, https://doi.org/10.1016/j.wear.2005.01.045.
6. Wrona et al., "Methodology of Testing Shot Blasting Machines in Industrial Conditions," Archives of Foundry Engineering, vol. 12, no. 3, pp. 145-148, 2012. DOI: 10.2478/v10266-012-0045-6.
7. P. GillströM, M. Jarl, Replacement of pickling with shot blasting for wire rod preparation, Scand. J. Metall. 33 (2004) 269–278, https://doi.org/10.1111/j.1600-0692.2004.00692.x.
8. X. Shi, Research of the influence of shot blasting cleaning on the surface roughness of iron casting, Foundry 62 (2013) 1241–1243, https://doi.org/10.3969/j. issn.1001-4977.2013.12.020.
9. H. Huang, F. Yang, Y. Gao, Numerical simulations on process and effectiveness of rust removal by shot blasting, Surf. Technol. 45 (2016) 194–201, https://doi.org/10.16490/j.cnki.issn.1001-3660.2016.11.030.
10. WILCOX, David C. Turbulence modeling for CFD. 3rd ed. La Canada, Calif.: DCW Industries, 2006. ISBN 978-1-928729-08-2.